Repeated failures of the giant Beshkiol Landslide and their impact on the long-term Naryn Basin floodings, Kyrgyz Tien Shan

Losen, J.; Rizza, M.; Nutz, A.; Henriquet, M.; Schuster, M.; Rakhmedinov, E.; Baikulov, S.; Abdrakhmatov, K.; Fleury, J.; Siame, L.

DOI
10.1016/j.geomorph.2024.109121

Publication date
2024

Document Version
Final published version

Published in
Geomorphology

Geomorphology 453 (2024) 109121

Contents lists available at ScienceDirect

Geomorphology

journal homepage: www.journals.elsevier.com/geomorphology

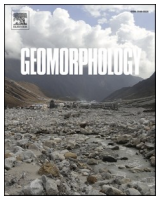

Repeated failures of the giant Beshkiol Landslide and their impact on the long-term Naryn Basin floodings, Kyrgyz Tien Shan

J. Losen [a,*], M. Rizza [a,b], A. Nutz [a], M. Henriquet [a,c], M. Schuster [d], E. Rakhmedinov [e], S. Baikulov [e], K. Abdrakhmatov [e], J. Fleury [a], L. Siame [a]

[a] Aix-Marseille Université, CNRS, IRD, INRAE, CEREGE, Aix-en-Provence, France
[b] Département des sciences de la Terre et de l'atmosphère, Université du Québec à Montréal, Montréal, QC H3C 3P8, Canada
[c] Department of Space Engineering, Faculty of Aerospace Engineering, Delft University of Technology, Delft, the Netherlands
[d] Université de Strasbourg, CNRS, ENGEES, Institut Terre et Environnement de Strasbourg, UMR 7063, 5 rue Descartes, Strasbourg, France
[e] Institute of Seismology, National Academy of Sciences of the Kyrgyz Republic, Kyrgyzstan

ARTICLE INFO

Keywords:
Landslide
Dammed-lake
Quaternary dating
Kyrgyzstan

ABSTRACT

Landslides are major hazards that lead to cataclysmic changes in regional physiography. Their consequences are particularly significant when they affect a river system, forming dammed-lake upstream that represents a high flood threat for the downstream region. The Naryn River is the largest river in the Kyrgyz Tien Shan and is of great economic importance. The Beshkiol Landslide, the largest one in Central Asia but of unknown age, has most likely blocked the Naryn River in the past during the Late Pleistocene, with evidence of thick lacustrine deposits as well as numerous paleo-shorelines preserved upstream. In this study, a detailed geomorphological and sedimentological analysis combined with luminescence and ^{14}C dating provides a strong chronological framework to refine the dynamics between the Beshkiol landslides and dammed-lakes in the Naryn Basin. We propose that the Beshkiol Landslide was first triggered 51.9 ± 4.4 kyrs ago, with a 410 m-high dam that blocked the Naryn River. A first lake with a total volume of 121 ± 50 km^3 lasted for >37.0 ± 5.1 kyrs, one of the longest landslide-dammed lake residence time ever documented in the world. Our sedimentological observations highlight a catastrophic lake outburst flood between 15.6 and 14.1 kyrs cal BP, likely related to a landslide dam breach. A short-lived phase of fluvial erosion impacted the whole Naryn Basin followed by a second landslide activation (280 m- high dam) and subsequent flooding by a second lake of 27 ± 10 km^3. This second lake had a minimum residence time of 7.7 ± 1.3 kyrs before its final gradual drainage that was followed by a fluvial erosional phase still active today in the Naryn Basin. We also suggest that the distal unconsolidated part of the Beshkiol Landslide could be remobilized in the event of an earthquake and/or extreme rain episode, causing a potentially dam of the Naryn River, which would have strong regional economic impacts.

1. Introduction

Landslides are one of the major natural hazards that claim thousands of direct casualties and damage infrastructures around the world every year. They can be triggered by earthquakes (Schuster and Alford, 2004; Xu et al., 2009), high-intensity precipitations (Weng et al., 2011; Yi et al., 2021) or strong climatic variations (Morino et al., 2019; Delgado et al., 2020). They may also have long-term impacts, especially when a landslide intersects a river system leading to upstream flooding of the valley and the creation of dammed-lakes. Also, catastrophic dam break flood represents a secondary major hazard and the associated erosive pulse strongly modifies the surrounding morphology and sediment budgets (Costa and Schuster, 1988; Goswami et al., 1999). There are well-documented historical examples of dammed-lakes around the world (Evans et al., 2011), but the geomorphological and sedimentological record of paleo-landslides and related paleo-lakes are much less studied, leading to an incomplete knowledge of their evolution scheme. Landslides are the first natural hazards impacting Central Asia mountain ranges (Strom, 2010; Havenith et al., 2013) and their volume can reach up to 10 km^3 (Strom and Korup, 2006). In this region, earthquakes are one of the main triggering factors, such as the magnitude Mw 7.4 1911 Pamir earthquake, which induced a landslide that dammed the Murgab

* Corresponding author.
E-mail address: losen@cerege.fr (J. Losen).

https://doi.org/10.1016/j.geomorph.2024.109121
Received 5 June 2023; Received in revised form 23 February 2024; Accepted 27 February 2024
Available online 6 March 2024

Valley with 2 km^3 rockslide debris, and whose filling is the origin of the 16 km^3 Sarez Lake (Schuster and Alford, 2004; Evans et al., 2011). The corresponding Usoi Dam reaches a height of 620 m above the riverbed, which makes it the world's largest dam (Ischuk, 2006).

Other massive landslides have been reported across the Tien Shan Range, and some of them induced very large dammed-lakes (Havenith et al., 2013, 2015), such as the Beshkiol Landslide, the largest of Central Asia. Located on the northern flank of the Akshiyriak Range (Fig. 1), the 7 km-long Beshkiol rockslide involved about 10 km^3 of material and formed a high dam that blocked the course of the Naryn River (Strom, 1998). Presently, the river left most of the landslide mass intact, cutting a narrow tortuous 10 km-long gorge at its foot. Upstream of the Beshkiol Landslide, horizontal terraces above the actual Naryn River also suggest lacustrine deposits in the Naryn Basin, likely related to the ancient dammed-lake (Strom and Korup, 2006).

However, besides these preliminary observations, several important questions remain unsolved. When was the Beshkiol Landslide originated? What was the extension of the resulting dammed-lake across the Naryn Basin and what have been the geomorphological consequences? How long did the dammed-lake span? What were the dynamics of emptying the lake? To answer these questions, detailed geomorphological, sedimentological, and chronological investigations were performed in the Naryn Basin and the Beshkiol area. The data obtained highlight a unique stratigraphic record over the past 50,000 years and suggesting a complex response of dammed-lakes to multiple activation phases of the Beshkiol Landslide. This study provides valuable new data for a better understanding of the long-term stability of dammed-lakes, a key information to improve landslide hazards assessment.

2. Study area

The western part of the Tien Shan (Fig. 1) is an active mountain range still absorbing the India-Eurasia convergence (Tapponnier and Molnar, 1979), with occurrence of large earthquakes (Mw > 7) (Kalmetieva et al., 2009; Rizza et al., 2019). In Kyrgyzstan, strong historical earthquakes have triggered important landslides, causing more victims than the seismic events themselves, such as the Mw 7.9 1911 Kemin and the Mw 7.8 1992 Suusamyr earthquakes (Fig. 1) (Delvaux et al., 2001; Grützner et al., 2019). In the Tien Shan, > 4000 landslides have been detected (Fig. 1) and some of them have been associated with the formation of dammed-lakes (Havenith et al., 2013, 2015).

The Naryn River represents an important economical asset in Central Asia as relatively large cities, hydroelectric infrastructures, and major water reservoirs have been built along its course. This river drains the 300 km-long Naryn Basin, one of the largest intramontane basins in the Kyrgyz Tien Shan (Fig. 1), bounded to the north and to the south by the 3500 m-high Moldo-Too and Baybeiche Ranges, respectively (Fig. 2a). This intramontane basin is marked by active thrust faults and folds that deformed Cenozoic strata up to Quaternary fluvial terraces (Thompson et al., 2002; Goode et al., 2014).

Along the Akshiyriak Range, the 8–12 km^3 Beshkiol mega-landslide is well identified on low-resolution satellite images analysis (Strom, 1998) as well as active fault segments (Figs. 1 and 2a). At the toe of the Akshiyriak Range, running from the Kazarman Basin up to the Beshkiol area, Holocene SSE-NNW striking normal fault scarps are interpreted as possibly resulting from fold bend extrado on a blind south-dipping reverse fault (Rizza et al., 2019). Active fault scarps, identified on both sides of the Beshkiol scar, favoured a seismic triggering of the landslide (Strom and Korup, 2006). However, no large historical or instrumental earthquakes have been recorded in the vicinity of the study

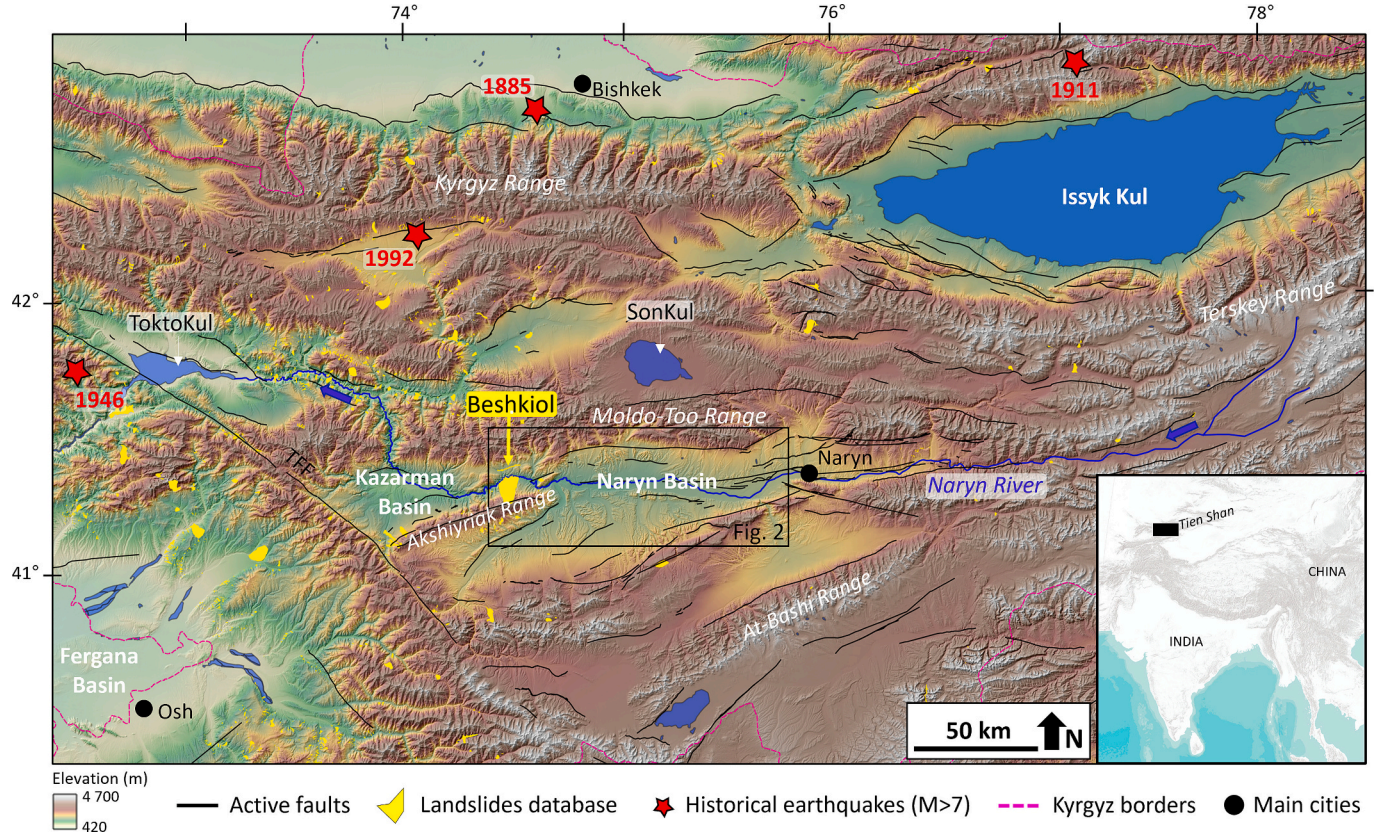

Fig. 1. Shaded relief of the study area, showing the Kyrgyz Tien Shan with active faults in black solid lines (modified after Rizza et al., 2019), major landslides in yellow (Havenith et al., 2015), large historical Mw > 7 earthquakes (Kalmetieva et al., 2009), major lakes in blue and main cities located by black dots. The black box locates the study area and Fig. 2. TFF = Talas-Fergana Fault.

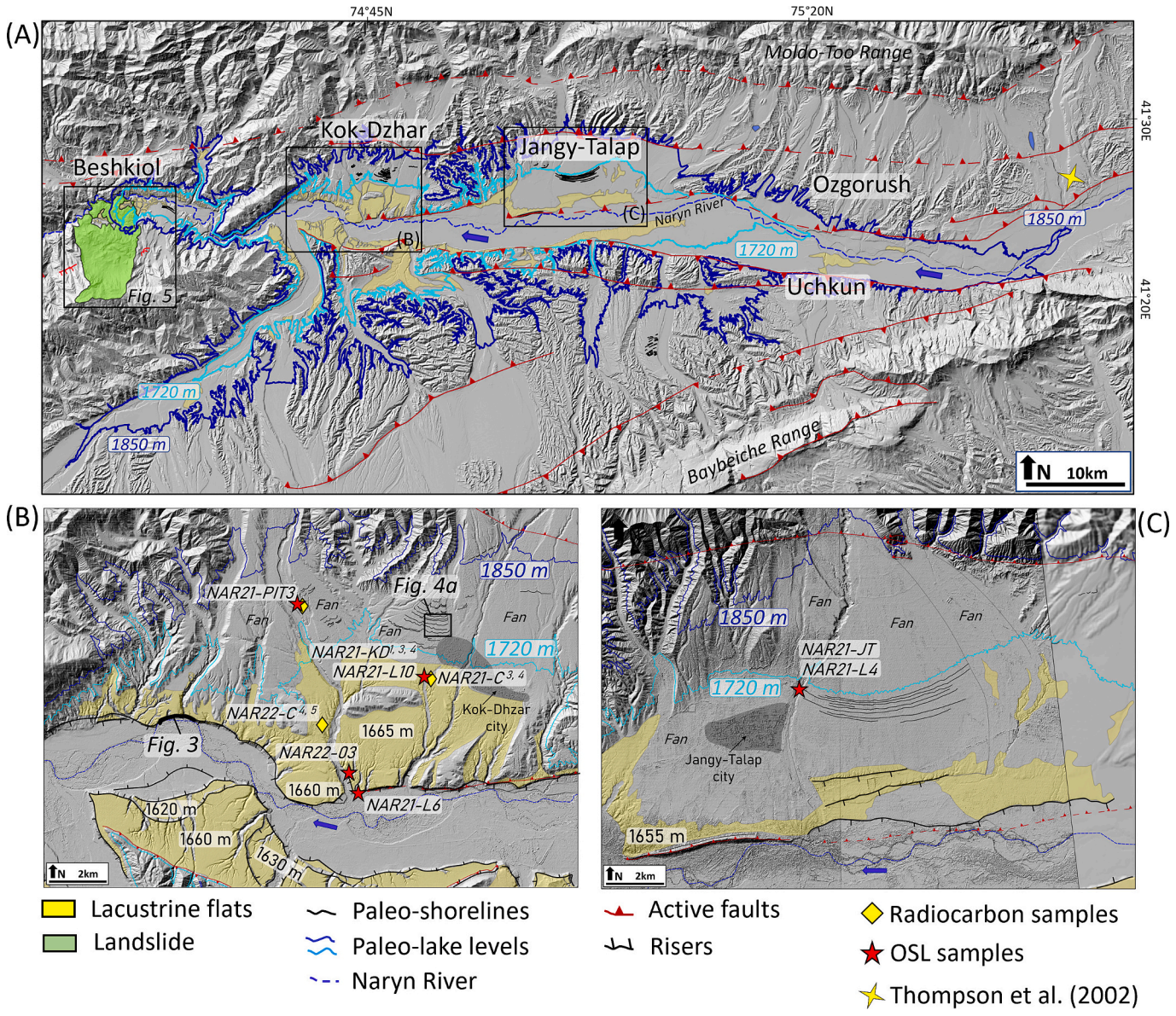

Fig. 2. A) Detailed mapping of lacustrine flats and paleo-shorelines from Beshkiol to Ozgorush on top of a hillshade FABDEM grid, with reconstruction of the approximate high lake levels at 1850 m in dark blue and at 1720 m in light blue. B) and C) are detailed views of the Kok-Dhzar and Jangy-Talap areas, respectively. OSL (red stars) and radiocarbon (yellow diamonds) sample locations are indicated. Light-yellow areas represent lacustrine deposits and the localisations of Figs. 3 and 4 are represented by a black box or a wide dark line on B, respectively.

area (Thompson et al., 2002; Goode et al., 2014; Rizza et al., 2019).

The upper part of the Beshkiol scar is initiated in Paleozoic rocks, forming a large 600 m-high and 1 to 1.5 km wide step in the morphology. The runout of the landslide, from the top of the main scar to the Naryn River, is estimated to be 8 to 10 km-long with a drop of 2.0 to 2.6 km high (Strom and Korup, 2006). The landslide body is mostly composed of bedded Neogene sandstone, siltstone and conglomerate blocks with gypsum interbeds, which originally formed a syncline (Strom, 1998, 2010). The landslide basal contact coincides with the base of the Neogene sequence. Presently, the Naryn River deeply incises the landslide (Chu Formation) and the bedrock (Devonian limestones) of the former right bank of the valley. It flows at the toe of the landslide and then crosses downstream to the Kazarman Basin (Fig. 1).

Previous studies proposed that the Beshkiol Landslide had formed a high dam over the Naryn River (Strom, 1998; Strom and Korup, 2006; Strom, 2010). Upstream the landslide, in the Naryn Basin, lacustrine sedimentation was proposed based on few observations on satellite images (Strom, 2010). The western Naryn Basin is locally known as "Ak Talaa" due to the prominence of white sedimentary units that may have accumulated in a paleo-lake as some observations of ancient shoreline berms rising above the white clay deposits (Goode et al., 2014) but no detailed studies of these structures have been conducted.

3. Materials and methods

3.1. High-resolution images, mapping and field observations

The geomorphic analyses are based on topographical data calculated from multi-stereoscopic Pleiades optical images that were used to generate a 1 m resolution Digital Surface Model (Fig. 2), complemented with the 30 m global map of elevation with forests and buildings removed (FABDEM, Hawker et al., 2022). The Pléiades stereo images (0.5 m spatial resolution) were processed with the Micmac workflow (Rupnik et al., 2017). These optical and topographical data allowed for a detailed mapping of the study area to identify alluvial and lacustrine terraces, alluvial fans, paleo-shorelines, slope failures and topographic

Table 1
OSL ages on quartz extracts and associated data for lacustrine sediments. Altitude represents the top surface and does not correspond to the sampling elevation. Number of aliquots in brackets represent the total running and without brackets those selected for age calculation. Equivalent doses are calculated using ADM (Guérin et al., 2017), while equivalent dose* is calculated using Minimum Age Model (MAM) (Galbraith and Roberts, 2012) at three parameters, with sigma_b of 0.11 ± 0.04.

Sample ID	Grain size (μm)	Localisation	Altitude (m)	Depth (m)	H_2O (wc% ± 2 %)	K (%)	Th (ppm)	U (ppm)	Gamma spectrometry (Gy/kyr)	Cosmic dose rate (Gy/kyr)	Dose rate (Gy/kyr)	Number of aliquots	De (Gy)	Age (yrs)
Beshkiol														
BESH22–04	100–63	41.43341 N 74.54867 E	1648	0.2	14	1.83 ± 0.18	9.43 ± 0.94	2.68 ± 0.40	–	0.322 ± 0.032	3.06 ± 0.16	24 (30)	49.25 ± 1.66	16,100 ± 990
BESH22–07	100–63	41.44861 N 74.52046 E	1640	2	15	1.87 ± 0.18	8.62 ± 0.86	4.33 ± 0.65	–	0.216 ± 0.022	3.24 ± 0.17	35 (36)	54.52 ± 1.51	16,830 ± 1000
BESH22–06	100–63	41.44540 N 74.51985 E	1568	40	17	1.59 ± 0.16	7.67 ± 0.77	2.58 ± 0.26	0.91 ± 0.05	0.015 ± 0.002	2.22 ± 0.12	41 (46)	115.01 ± 7.42*	51,880 ± 4395*
Kok-Dhzar														
NAR21-PIT3	100–63	41.46898 N 74.78032 E	1761	1.6	17	0.75 ± 0.07	3.26 ± 0.33	1.75 ± 0.17	0.35 ± 0.21	0.228 ± 0.023	1.34 ± 0.07	29 (31)	9.56 ± 0.79	7590 ± 730
NAR21-LI10	140–100	41.4526 N 74.8210 E	1703	2	15	0.94 ± 0.09	6.20 ± 0.31	2.81 ± 0.28	0.86 ± 0.05	0.219 ± 0.022	2.08 ± 0.09	62 (81)	17.39 ± 0.47	8840 ± 460
NAR22-03	180–63	41.42805 N 74.79583 E	1653	15	17	2.16 ± 0.21	12.00 ± 0.60	3.34 ± 0.33	–	0.062 ± 0.006	3.24 ± 0.18	18 (25)	49.05 ± 1.78	15,150 ± 1000
NAR21-L6	11–4	41.42333 N 74.79901 E	1630	56	11	2.12 ± 0.21	9.88 ± 0.90	2.88 ± 0.28	–	0.008 ± 0.001	3.27 ± 0.18	9 (10)	109.82 ± 10.26	33,540 ± 3620
Jangy-Talap														
NAR21-L4	100–63	41.46723 N 75.03415 E	1718	0.65	16	1.54 ± 0.15	7.70 ± 0.38	2.34 ± 0.23	–	0.268 ± 0.027	2.40 ± 0.12	26 (40)	17.96 ± 1.28	7490 ± 650
NAR21-JT	100–63	41.46724 N 75.03409 E	1716	1.3	16	1.28 ± 0.13	6.78 ± 0.34	2.10 ± 0.21	0.54 ± 0.03	0.239 ± 0.024	1.88 ± 0.10	34 (34)	29.90 ± 0.38	15,890 ± 845

fault scarps. This remote sensing analysis was also completed by field surveys conducted in the Naryn Basin and on the Beshkiol Landslide during two campaigns in 2021 and 2022. Lithology, grain size, sorting, bed thickness, sedimentary structures, and paleocurrents were assessed based on conventional facies analysis. Drone flights on remote areas or along vertical cliffs enabled establishing the relative stratigraphy of the different units and analysing their architectures (supplementary material S1).

3.2. Luminescence dating

Nine samples were collected for Optically Stimulated Luminescence (OSL) dating within sandy to silty lacustrine sediments, after a clean off along the outcrop, by hammering of metal tubes. Under subdued red-light conditions, samples were treated following classical chemical procedures to separate quartz grains for OSL dating (Wintle, 1997).

The total uranium (U), thorium (Th), potassium (K) and rubidium (Rb) contents of the samples were determined (see Table 1) from subsamples of the sampling tubes using inductively-coupled plasma mass spectrometry (ICP-MS) carried out at the Service d'Analyse des Roches et des Matériaux (SARM, France). Elemental concentrations were converted to dose rates using the conversion factors of Liritzis et al. (2013), the appropriate adjustments for grain size attenuation (Guérin et al., 2012) and the sample water content (Adamiec and Aitken, 1998) (see Table 1). A portion of the inner tube was used to estimate of "in situ" maximum saturation water content (H_2O wc% in Table 1) using the syringe method (Murray et al., 2021). The cosmic dose rates were determined based on the present sample depths and are shown in Table 1. The determination of the external gamma dose rate was obtained using a field gamma spectrometer Canberra InSpector1000 equipped with a 1.5 × 1.5 in IPRON-1 NaI probe. The processing of the spectra was done using the R gamma package (Lebrun et al., 2020).

All luminescence measurements were performed at Centre Européen de Recherche et d'Enseignement des Géosciences de l'Environnement (CEREGE, France) on a Lexsygsmart TL/OSL reader equipped with blue (458 nm, 90 mW/cm^2) and infrared (850 nm, 200 mW/cm^2) LEDs for stimulation, Delta-BP 365/50 EX and Hoya U-340 filters for light detection in the 330 nm to 390 nm bands. Measurements were conducted following the single-aliquot regenerative-dose (SAR) protocol (Wintle and Murray, 2000). Our applied acceptance criteria were 10 % recycling ratio and maximum recuperation of 5 %. The models for equivalent dose (De) distributions were performed with the Average Dose Model (ADM, Guérin et al., 2017) and final age calculations were compiled with the Dose Rate and Age Calculator (DRAC, Durcan et al., 2015; Kreutzer et al., 2016). All age determinations are summarised in Table 1.

3.3. Radiocarbon dating

Radiocarbon dating was also performed on eight detrital charcoals and shells collected in lacustrine units and from some OSL sampling tubes. Chemical pretreatment and target preparation follow the methodology from Dumoulin et al. (2017) and Moreau et al. (2013). Radiocarbon samples were graphitized and analysed at the ARTEMIS ^{14}C Accelerator Mass Spectrometer (AMS) Facility (Saclay, France). Radiocarbon ages were calculated according to Mook and Van der Plicht (1999) by correcting the fractionation with the δ^{13}C calculated from the ^{13}C/^{12}C ratio measured on ARTEMIS. The δ^{13}C used includes fractionation occurring both during sample preparation and during the AMS measurements. Finally, each individual age was calibrated using OxCal software version 4.4.4 (Ramsey, 2009) and the Intcal20 calibration curve (Reimer et al., 2020). All age determinations are summarised in Table 2.

4. Results

4.1. Naryn Basin

4.1.1. Geomorphic markers

In the Naryn Basin, the lacustrine sedimentary deposits are well identified from Kok-Dhzar to Ozgorush, with a lateral extension of over 65 km (Fig. 2a). At the longitude of Jangy-Talap until Ozgorush, lake deposits are increasingly scattered and poorly preserved (Fig. 2a and c). At the longitude of Kok-Dhzar, they are particularly well-preserved on both banks of the Naryn River, in the central part of the basin (Fig. 2b). These deposits are now perched up to ~100 m above the present Naryn riverbed (~1565 m), indicating a significant river incision phase after the lake was drained. The geometry and nature of these deposits are detailed in Section 4.1.2 and in Fig. 3. Flat longitudinal slopes characterise lacustrine terraces from wave-action in the nearshore. They are distinguished from river terraces, which have a similar slope as the Naryn River (0.29 %). In the topography, these flats highlight redundant altitudes forming paired terraces at 1690 m, 1660 m, 1630 m and 1590 m from Kok-Dhzar to Jangy-Talap. At Uchkun and Ozgorush, lacustrine deposits can reach an elevation of 1815 m (Fig. 2a).

Above the lacustrine deposits, multiple whitish and silty features corresponding to 50 cm to 1 m-high curvilinear ridges were observed, following topographic contour lines over a distance of hundreds of meters (black lines in Fig. 2). These features, recognized from satellite imagery and field observations, can be interpreted as regressive paleo-shorelines overlying alluvial fans (Fig. 4a). Two clusters of shorelines are identified at different altitudes in Kok-Dhzar and Jangy-Talap (Fig. 2b and c, respectively). At Kok-Dhzar, a series of 22 benches were mapped between 1780 m and 1730 m and 4 poorly preserved shorelines were found between 1850 m and 1800 m. At Jangy-Talap, a clustering of 9 beach ridges, a few kilometer-long and 1 to 2 m-high, were mapped between 1715 m and 1695 m (Fig. 4a) and several discontinuous and poorly preserved benches were found between 1840 m and 1735 m on perched alluvial fans. The continuity of theses paleo-shorelines is often hindered by anthropogenic irrigation channels and agricultural lands.

4.1.2. Sedimentological analyses

At Kok-Dhzar, a 2 km-long cliff along the Naryn River (Fig. 3a and supplementary material S1) allows to observe and delineate several sedimentary units. In the following, sediment units (U) are described and interpreted considering that each unit corresponds to an accumulation of sediments with a uniform lithology, although they may show lateral changes in facies or facies associations and limited by unconformities or correlative conformities. Interpretation of sediment units provides evolution of sedimentary environments in the central portion of the Naryn Basin during the considered time interval.

U0 corresponds to the basement of the investigated sedimentary succession and marks the pre-Quaternary basement of the Naryn Basin (Goode et al., 2011). This unit is the Neogene Chu Formation (Abdrakhmatov et al., 2001) and is exposed all over the Kyrgyz Tien Shan. U0 is made of grey-green laminated muds revealing regional long-term lacustrine conditions before Kyrgyz Tien Shan uplift. It shows 10° to 20° dipping stratas (Fig. 3c) that illustrate a post-depositional tilting. The top boundary intersects master beds forming toplap termination; it is uneven with 30–40 m differences between highs and lows, which underlines the development of relatively deep incisions prior to the Quaternary sedimentation. All Quaternary sediments presented afterwards are unconformably overlying the Chu Formation.

U1 consists of clast-supported conglomerates (Fig. 3b) in hundred meters wide and tens meters thick lobes. Along the cliff, where U1 is not affected by subsequent erosion, the top boundary is slightly convex progressively pinching out laterally. Where it is observed, U1 deposited in incision at the top of U0. In the western part of the Naryn Basin, remnants of conglomeratic beds are also observed on top of the Chu Formation, and are interpreted as alluvial fans directly overlying U0.

U2 is a 10 to 70 m thick unit dominated by muds overlaying either U0 or U1 (Fig. 3b and c). In its lower part, U2 includes laminated muds with occasional current ripples in sandy layers, sparsely intercalated by meter-scale beds with clast-supported coarse to very coarse gravel. Upward, gravelly beds progressively disappear and horizontally-laminated muds prevail. In the upper part, muds show a progressive transition from horizontal to undulated stratifications with 10–20 m wavelength. In places, pseudo-foresets dipping downstream are observed. At the top, U2 shows moderately developed paleosoils. The top boundary of U2 is undulating with 1–10 m differences between highs and lows, indicating a significant erosion episode. U2 reveals a lacustrine environment and the establishment of a perennial paleolake in the Naryn Basin. Horizontally-laminated muds indicate deposition from settling in a subaqueous environment while current ripples suggest occasional bottom currents. Sparse conglomerates in the lower part of U2 reveal occasional dense debris flows likely fed by river flows which entered the lake during flood episodes. In the middle part of U2, the lake enlarged and low-energy sedimentation prevailed with a limited impact of lake margin processes. In the following, U2 will be referred to as the "Erkin formation", it constitutes a first lake formation. In the upper part of U2, transition from horizontal to undulating laminations with pseudo-foresets evidence the transition from low-energy environment to conditions dominated by permanent supercritical unidirectional currents, revealing an intense increase of the flow velocity. Undulating strata and pseudo-foresets document short-wavelength (10–20 m) cross-strata related to transport toward the Beshkiol gorge by either stable anti-dunes or cyclic steps (Cartigny et al., 2011, 2014). Afterwards, this part of U2 will be referred to as the "Henriquet Flush Event" (HFE). Subsequently, paleosoils and the uneven upper boundary of U2 indicate an emersion and a significant post-depositional erosional phase.

U3 is 1 to 20 m thick, mostly made of laminated muds, and erosionally overlies U2 (Fig. 3b and c). U3 shows a facies succession broadly comparable to U2. In the lower part, muds dominate even if frequent meter-scale beds with clast-supported gravels are observed. Equivalently to U2, gravels disappear upward where horizontally-

Table 2
Calibrated radiocarbon ages at 2σ from charcoal, bulk and shell samples and associated data in the Kok-Dhzar area.

Sample ID	Sample lab ID	Localisation	Altitude (m)	Organic component	δ^{13}C PDB (‰)	pMC	^{14}C age (yrs BP)	^{14}C age (yrs cal BP)
NAR21-PIT3-GN	A66582	41.46898 N 74.78032 E	1766	Shell (Gibbulinopsis nanosignata)	−4.00	42.128 ± 0.122	6945 ± 30	7910–7685
NAR21-KD4	A66577	41.45261 N 74.82109 E	1704	Charcoal	−26.00	37.875 ± 0.170	7800 ± 35	8640–8450
NAR21-KD1	A66575			Charcoal	−28.30	37.325 ± 0.166	7915 ± 35	8980–8600
NAR21-KD3	A66576			Charcoal	−22.60	37.083 ± 0.164	7970 ± 35	8990–8650
NAR21-C3	A66578	41.44952 N 74.82069 E	1684	Enriched OM level	−28.50	28.868 ± 0.157	9980 ± 45	11,690–11,260
NAR22- C5	A70265	41.43872 N 74.78764 E	1664	Charcoal	−20.20	22.456 ± 0.198	12,000 ± 70	14,065–13,615
NAR22-C4	A69135			Charcoal	−24.00	21.873 ± 0.152	12,210 ± 60	14,785–13,880
NAR21-C4	A66579	41.44952 N 74.82069 E	1670	Enriched OM level	−27.80	21.617 ± 0.147	12,300 ± 50	14,810–14,075

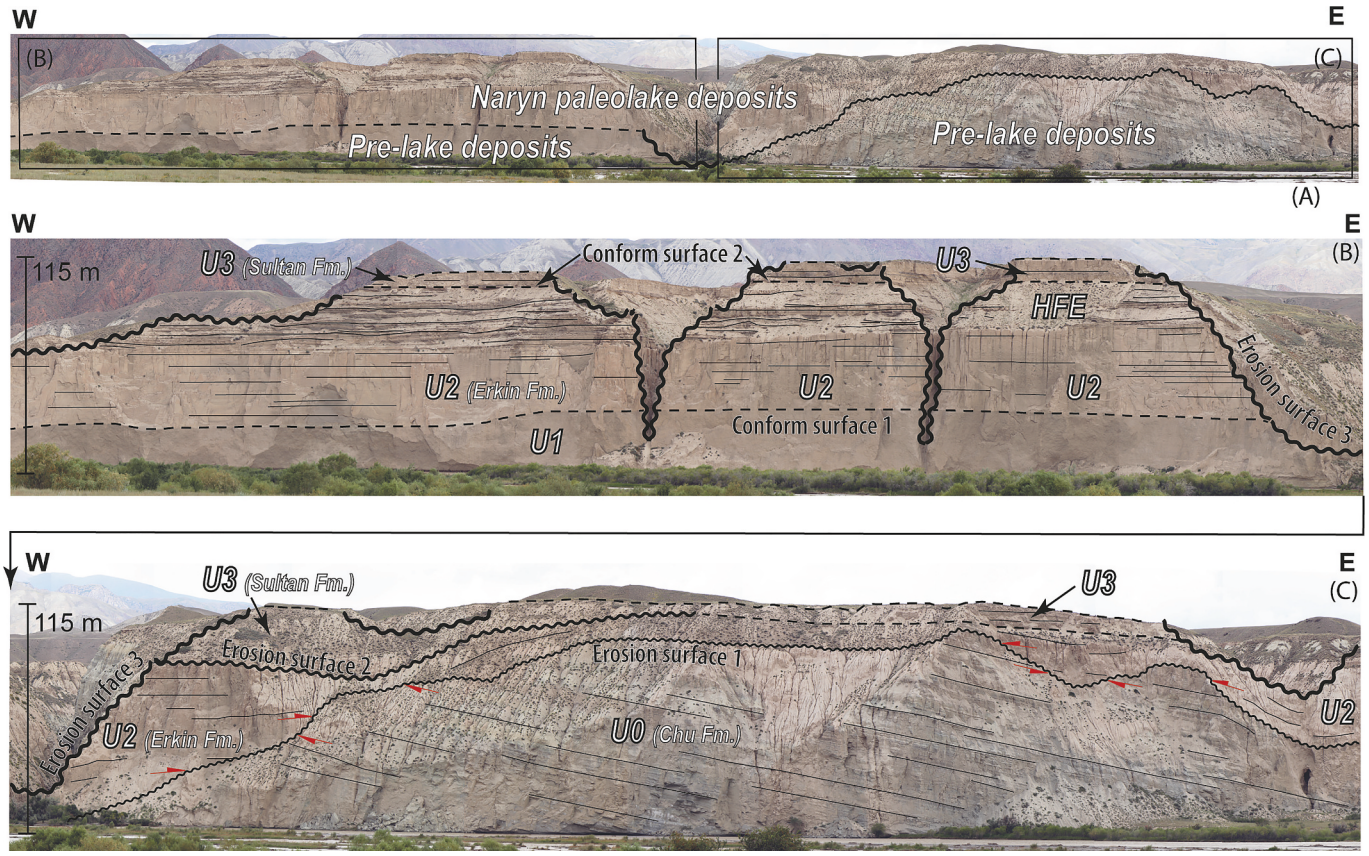

Fig. 3. A) Panoramic view of the studied cliff along the Naryn River showing the succession of lacustrine sequences south-east of Kok-Dzhar (location on Fig. 2b). This cliff was surveyed by a drone flight presented in supplementary material S1. B) and C) Large-scale sedimentary architectures of lacustrine sequences which are zooms of A. We can observe 4 sedimentary units: U0 which corresponds to the Chu Formation and U1 which corresponds to an ancient alluvial fan. These two units are separated from the overlying unit by an erosion surface (erosion surface 1). Above these units, a first lacustrine unit (U2, Erkin Formation) is identifiable, and its upper part is marked by undulating laminations (HFE). Separated from U2 by an erosion surface (erosion surface 2), a second lacustrine unit has been identified (U3, Sultan Formation), the top of which is marked by current erosion (erosion surface 3).

laminated muds prevail. A major difference with U2 is that U3 does not show evidence for supercritical flows in the upper part. The upper boundary of U3 is an uneven surface, and well-developed paleosoils are observed. In the following, U3 will be referred to as the "Sultan formation", it constitutes a second lake formation. The lower part records the establishment of lacustrine conditions with episodic debris flows and hyperpycnal flows during particularly powerful flood episodes. Above, perennial low-energy lacustrine conditions were progressively established. In the uppermost part, paleosoils evidence subsequent emersion and drying of the previous lake. The uneven top surface reveals a subsequent erosional phase that formed the present-day topography.

The sequence of deposits observed at Kok-Dhzar extends seamlessly to the Uchkun and Ozgorush areas. At elevations ranging from 1765 to 1800 m, we identified a continuous base contact characterized by the Chu Formation being tilted, overlain by fluvial deposits resting on an erosive base, followed by unconformable lacustrine deposits (Fig. 3). It's noteworthy that the lacustrine deposits at Uchkun/Ozgorush outcrop at higher elevations than those observed at Kok-Dhzar or Jangy-Talap, which are approximately 1725 m.

4.2. Beshkiol area

4.2.1. Geomorphic markers and sedimentological analyses

The giant Beshkiol Landslide has left a spectacular morphological imprint in the northern flank of the Akshiyriak Range and has deeply modified the surrounding landscape (Fig. 5). The main body of the landslide (mb in Fig. 5a) has an altitude range from 1950 to 2240 m and covers an area of 25 km^2. Composed of blocks torn from Neogene and Devonian sedimentary units, the main landslide has left scars some 5 km-long and 350 m-high atop the Akshiyriak Range (main scars on Fig. 5a). The distal part of the main body is also delimited by a steep, 6 km-long and 360 m-high scar, starting point for the secondary sliding of multiple bodies (secondary scars on Fig. 5a). Along the left bank of the Naryn River, one of these masses of Chu Formation reaches a maximum elevation of 1750 m and spreads over >3 km-long (Fig. 4c), in sharp erosive contact with the bedrock composed of either Devonian limestones or Shamsi conglomerate Formation (Fig. 4d and supplementary material S1). Along the right bank of the Naryn River, over 2.5 km-wide of slipped volumes of Chu formation also unconformably overly the Devonian bedrock, strongly suggesting that the landslide crossed and blocked the Naryn Valley (Figs. 4c and 5c).

The estimations of dam heights are based on the maximum elevation of the shorelines identified at Kok-Dhzar and Jangy-Talap, and on the paleo-elevation of the Naryn River before the dams were formed. To evaluate the thickness of the dams, we used our field observations and the high-resolution DEM. Firstly, at Jangy-Talap, the cluster of shorelines represents the former regression levels of the second lake, with a maximum apparent water level at about 1720 m. This also corresponds to the minimum height for the second dam to allow water filling. Additionally, the secondary landslide mass reaches elevations of 1715 to 1750 m (Fig. 4d), which agrees with a water level at a minimum elevation of about 1720 m. At Kok-Dhzar, the cluster of shorelines represents the former regression levels of the first lake, with an apparent maximum water level at about 1850 m. Lacustrine deposits hanging between 1765 and 1816 m in Uchkun and Ozgorush areas (Fig. 2a) are higher than the maximum elevation of the second dam (1720 m),

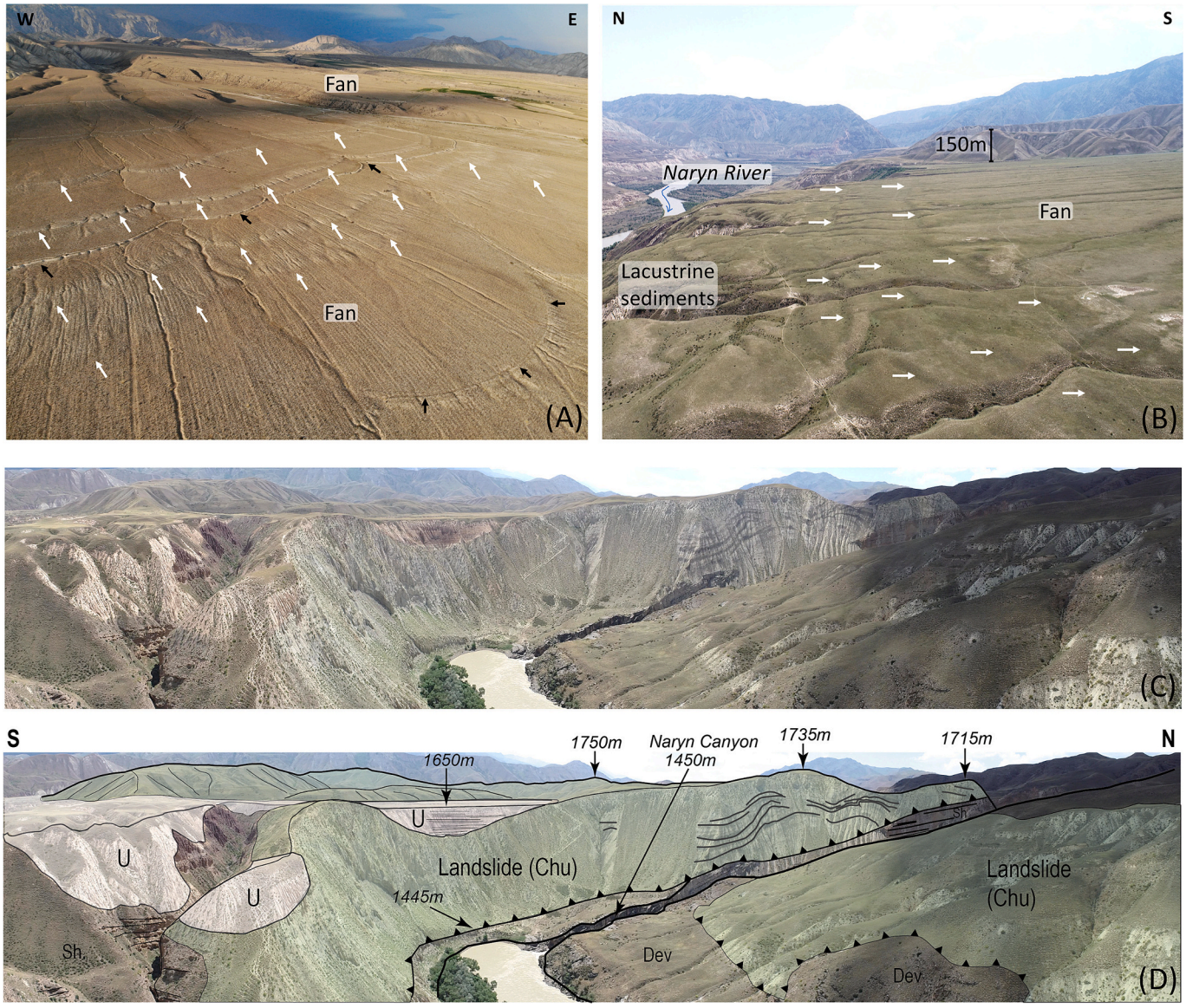

Fig. 4. Geomorphological markers and stratigraphic relationships of the landslide and lacustrine deposits. Oblique aerial (drone) photos of paleo-shorelines at Kok-Dhzar (A) and at Beshkiol (B). White arrows point to successive paleo-shorelines whereas black arrows point to man made irrigation channels. C) and D) Panoramic views of one of the secondary sliding masses which have potentially dammed the Naryn River. This view is taken from the drone flight presented in supplementary material S1. U = lacustrine units, Dev = Devonian rocks, Sh = Shamshi Formation and Chu = Chu Formation. Black triangles indicate the base of the landslide mass, overthrusting locally the bedrock.

indicating that the first lake had a higher water level.

Secondly, since the contact between the base of the Beshkiol Landslide with the Paleozoic basement is observed along the present-day riverbed (Fig. 4d), we thus consider that the present-day elevation of the Naryn River (~1440 m) is close to that before the damming. In this case, the difference between the elevation of the paleo-shorelines at 1720 m and the present-day Naryn River thus represents a minimum value of 280 m for the second dam's height. For the first dam, the paleo-shorelines being observed at about 1850 m, a minimum dam thickness of roughly 410 m can be estimated.

The lacustrine deposits were also recognized upstream of the Beshkiol Landslide (Fig. 5a). These deposits are located against and in front of the secondary landslides and have a lateral extension of over 3 km upstream of the landslide area. Fig. 4c shows light-coloured laminated silts overlying landslide deposits and bedrock units. Flat longitudinal slopes with some redundant altitudes were identified, forming paired terraces at 1690 m, 1650 m and 1615 m, at a lower elevation than the landslide ridges (Fig. 4c). In addition, 4 regressive paleo-shorelines, between 1650 m and 1630 m, were identified on top of an alluvial fan located 2.5 km upstream of the landslide mass (Figs. 4b and 5).

In the Beshkiol area, difficult access to the cliffs has limited our field observations. Laminated muds are preserved on the right bank of the Naryn River but the limited extension of the outcrops prevents a precise analysis of the sediment geometry and the two major lacustrine units (Erkin and Sultan Formations) are therefore poorly distinguished. The lacustrine sediments fill in the paleotopography of the surrounding landforms, as evidenced by the abnormal contact with the landslide bodies and the incised bedrocks (Fig. 4c and d).

4.3. Age controls

To understand the timing of the Beshkiol Landslide and its relation with the lake sediments, 17 ages have been obtained by luminescence and radiocarbon dating methods (Tables 1 and 2, Fig. 6). The

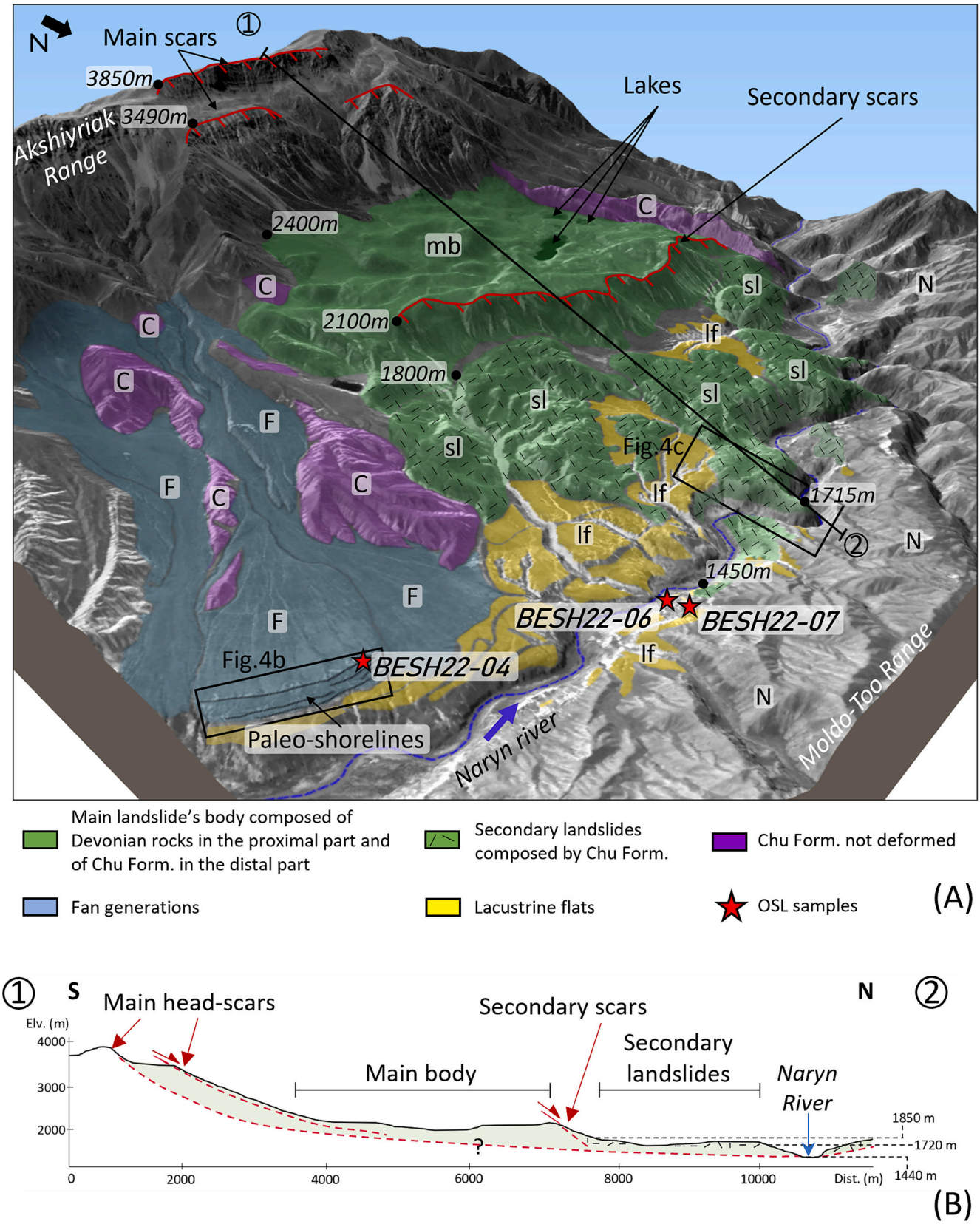

Fig. 5. A) 3D view of the Beshkiol Landslide with Pléiades orthophoto (© CNES (2021) and Airbus DS (2021), all rights reserved. Commercial use prohibited) showing all the features composing the landslide and its environment, mb = main body, sl = secondary landslide, lf = lacustrine flats, N = Neogene, C = in-situ Chu Formation, F = Fan. OSL sample locations are indicated by red stars. This figure allows to understand the complex morphology of the different events that have built the landscape. It is localised in Fig. 2. B) Topographic profile across the Beshkiol Landslide showing the different scars and their potential connection with a basal level (vertical exaggeration of x0.5).

geomorphological mapping and stratigraphic analysis from field outcrops revealed at least two major damming episodes. (See Figs. 6 and 7).

At Beshkiol, sample BESH22–06 (OSL) is the deepest sample (1569 m a.s.l) and was collected a few centimeters above the Paleozoic basement, in lacustrine beds filling an ancient paleotopography, at the toe of the landslide. This sample yielded an age of 51,880 ± 4395 yrs., post-dating the first phase of the giant Beshkiol Landslide, but it may be considered as a maximum age since the scattered equivalent doses distribution suggests unbleached grains. At Kok-Dhzar, sample NAR21-L6 (OSL), stratigraphically above BESH22–06, was collected in the lower part of the Erkin Formation and yielded an age of 33,540 ± 3620 yrs. BESH22–04, BESH22–07 and NAR22–03 samples (OSL) collected at the top of the Erkin Formation gave ages of 16,100 ± 990 yrs., 16,830 ± 1000 yrs. and 15,150 ± 1000 yrs., at Beshkiol and Kok-Dhzar respectively. The NAR22–03 sample was collected only 2 m below the HFE unit, which marks the end of the depositional phase of the Erkin Formation.

Samples NAR21-C4, NAR22-C4 and NAR22-C5 were both collected at the base of the Sultan Formation at Kok-Dhzar, with radiocarbon ages of 14,810–14,075 yrs. cal BP, 14,785–13,880 yrs. cal BP and 14,065–13,750 yrs. cal BP respectively, all post-dating the HFE unit. NAR21-C3 was also collected within the Sultan Formation, ~14 m above NAR21-C4, and gave a radiocarbon age of 11,690–11,260 yrs. cal BP. In the upper section of the Sultan Formation, ~2 m below the present surface, three radiocarbon samples (NAR21-KD4, NAR21-KD3, NAR21-KD1) gave ages ranging from 8990 yrs. cal BP to 8450 yrs. cal BP. These radiocarbon ages agree with the OSL age of 8840 ± 460 yrs. from the NAR21-L10 sample (Kok-Dhzar). Collected within alluvial fan sediments interbedded with the upper part of Sultan Formation, samples NAR21-PIT3 (OSL) and NAR21-PIT3-GN (^{14}C) yielded ages of 7590 ± 730 yrs. and 7910–7590 yrs. cal BP, respectively. These samples mark the end of the Sultan Formation at Kok-Dhzar.

At Jangy-Talap, sample NAR21-JT (OSL) was taken from a large alluvial fan dated at 15,890 ± 845 yrs. This fan is in a stratigraphic position below a silty berm (1715 m a.s.l), which indicates that the lake water was still present at this altitude to mark the topography. A sample collected in this berm yielded an OSL age of 7490 ± 650 yrs. (NAR21-L4).

4.4. Basin-scale evolution

These new geomorphic, sedimentological and chronological data allow the reconstruction of the complex relationships between the landslides in the Beshkiol gorge and the lake developments in the Naryn Basin (Fig. 7).

The oldest lacustrine deposits suggest that the first landslide episode occurred around 51,880 ± 4395 yrs. ago and blocked the Naryn River with a 7 km-wide and 410 m-high dam. Consequently, a first large lake filled up and the former fluvial valley upstream of the Beshkiol area up to the Naryn Basin was impounded. Sediments of the Erkin Formation deposited during this first lacustrine phase sealed the pre-landslide fluvial topography. Later, the lake quickly regressed followed by a short and catastrophic discharge (HFE) due to the break of the dam. This emptying phase induced a base-level drop that led to incisions of rivers and subsequent erosion of the lacustrine sediments and of the Beshkiol dam. During this erosive phase, the simultaneous failure of the entire front of the initial landslide from the secondary scars affected the foot of the former landslide, creating a second dam in the newly formed channel. This second landslide episode blocks the Naryn River for the second time with a 2 km-wide and 280 m-high dam. This chronology was refined by including stratigraphic information in the process of calibrating the ^{14}C and OSL ages using the Bayesian Oxcal calibration software (Ramsey, 2008). We ran a simple Bayesian model with two organized sequences (Erkin Fm and Sultan Fm) separated by one event. This event includes the first dam break (HFE), the erosional phase and the second dam activation. The 95.4 % PDF (probability density function) for this period ranges between 15,640 and 14,155 yrs. cal BP. We then estimate that the first lake occupied the Naryn Basin for a period of 36,980 ± 5140 yrs.

Following the secondary landslides, lacustrine conditions re-established and were at the origin of the Sultan Formation. This second lake occupied the Naryn Basin, started to decline around

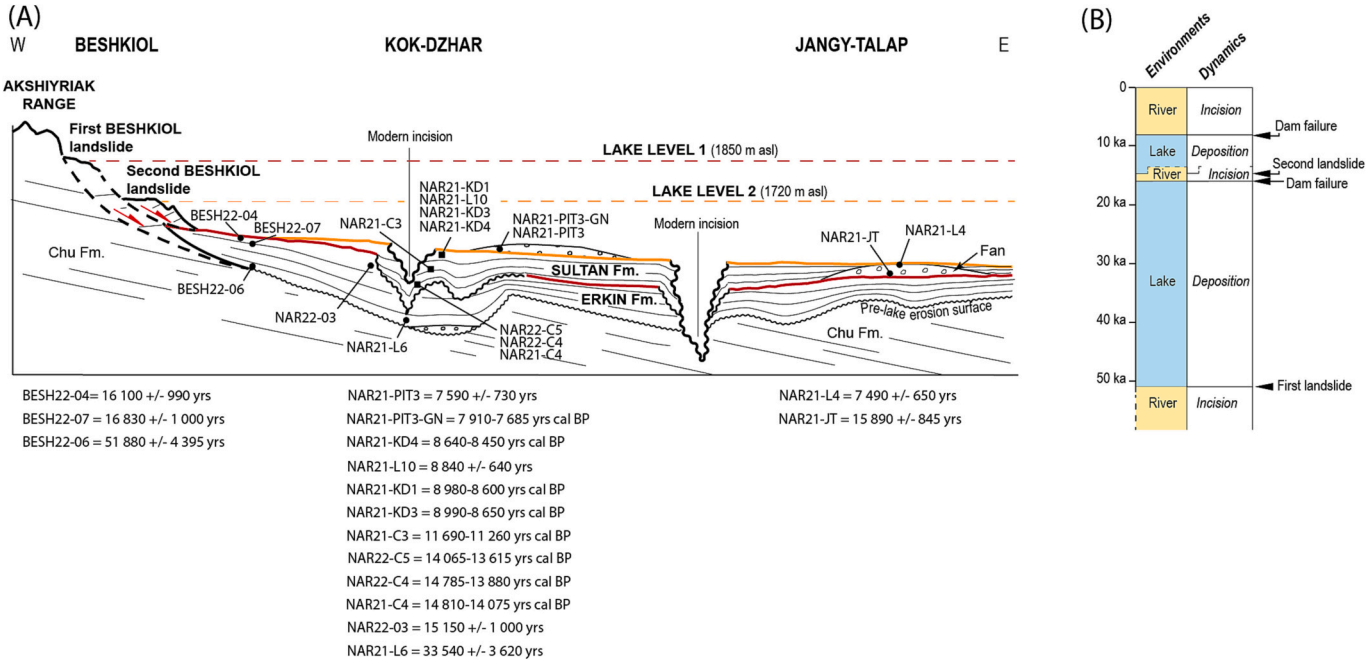

Fig. 6. Idealized basin-scale architecture and stratigraphy of the Naryn Basin deduced from our investigations (not to scale). A) Simplified cross-section showing the lacustrine Erkin and Sultan Formations in relation to the Beshkiol landslides. Black squares are for ^{14}C samples and black dots are for OSL samples. B) Pseudo-wheeler diagram for the last 60 ka in the Naryn Basin revealing that lacustrine conditions due to Beshkiol landslides significantly prevailed during this time interval.

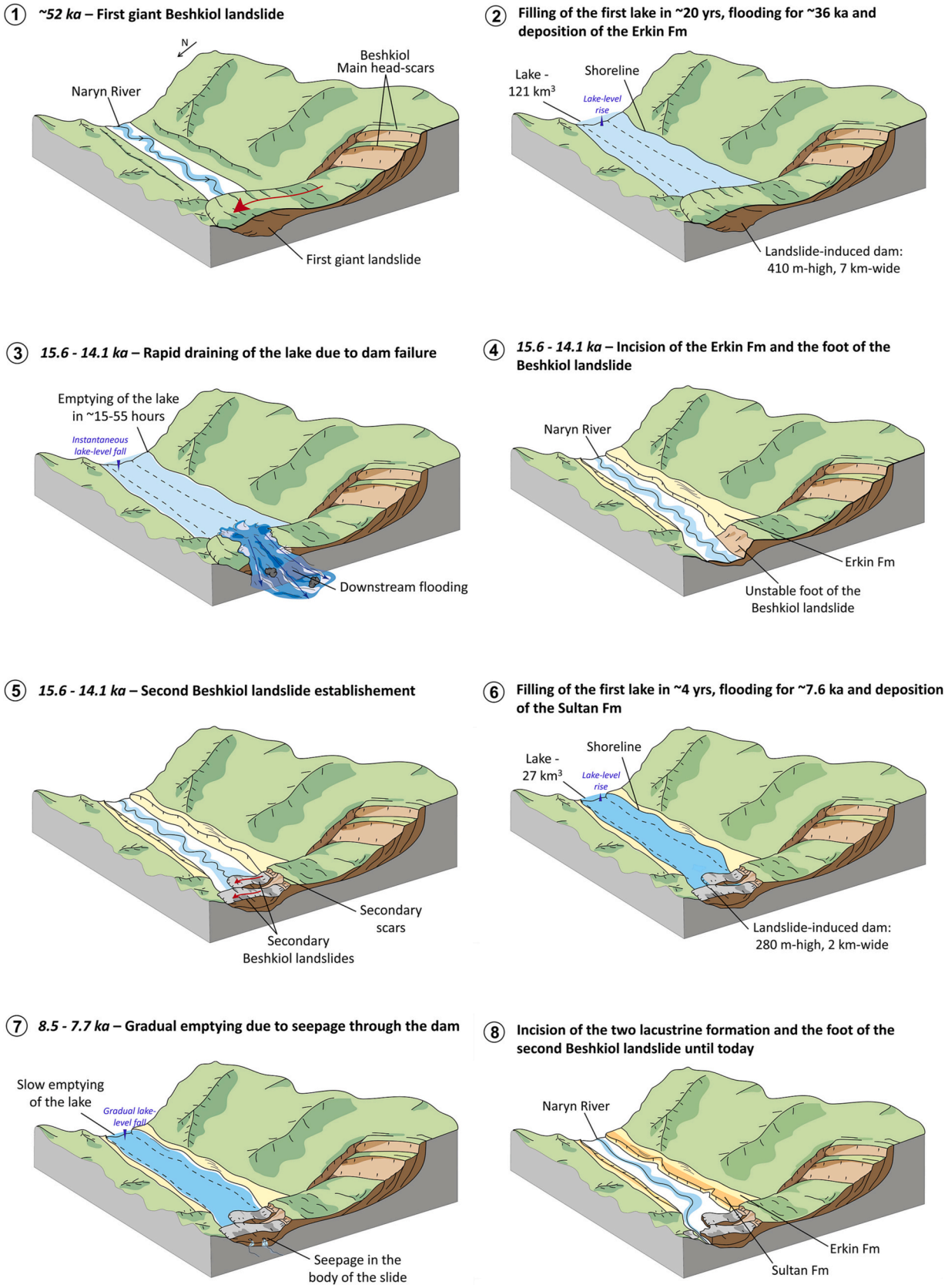

Fig. 7. Conceptual scenario for the geomorphological evolution of the Naryn Basin and Beshkiol Gorge. (1) Triggering of the first giant landslide around 52 kyrs. (2) Establishment of lacustrine conditions until 15.6 kyrs just before the rapid draining of the first dammed-lake in (3). (4) illustrates the fluvial conditions before second landslide events happened at 14.7–14.1 kyrs in (5). (6) shows lacustrine conditions until 7.5 kyrs and (7) the slow emptying of the second dammed-lake. (8) represents the modern morphology.

8560–7775 yrs. cal BP (determined by the Bayesian model), leading to a minimum residence time of 7675 ± 1285 yrs. Since then, the Naryn River and its tributaries incised both the Erkin and Sultan Formations as well as the bedrock, shaping the current topography with multiple flat levels and fluvial terraces.

5. Discussion

5.1. Duration of the lacustrine conditions in the Naryn Basin

Although the Beshkiol Landslide is the largest of Central Asia, it has not been dated until now. The obtained ages from the oldest lacustrine sediments suggest that the landslide was activated at least in the late Pleistocene, between 56,275 and 47,485 years ago. A compilation of modern and paleo-landslide dams showed that their longevity can range from only a few minutes to several thousand years (Alden, 1928; Ermini and Casagli, 2003). Their lifetime is mainly controlled by their shape, volume, grain size distribution, lithology, internal structure and the river flux (Weidinger, 2011), which are often poorly constrained due to the difficulty of characterising them for paleo-landslides. Previous studies based on the present day Naryn flux suggest that the Beshkiol landslide dammed the Naryn River and formed a 70 km-long lake that lasted about 3000 years (Korup et al., 2006; Fan et al., 2020).

Our sedimentological investigations highlight a more complex stratigraphic record over the past 50,000 years with two successive major dam episodes and associated lakes. The first lake lasted for 36,980 ± 5140 yrs., which led to a long-term change in the dynamics of the Naryn River. From our morphological observations, it can be proposed a maximum expansion of this lake up to an elevation of 1850 m (dark blue line at 1850 m in Fig. 2a), corresponding to a 100 km-long and 20 km-wide lake (~1100 km^2) with a minimum estimated volume of 121 ± 50 km^3 (calculated with QGIS and a DEM of the current topography). The high stability of the first dam could be explained by its exceptional size (> 7 km long, 10 km^3). If this first lake remained stable for >36,980 ± 5140 yrs., it is necessary to assume that the outflow of water through the dam plus the evaporative capacity of the lake at the time were equal to the inflow from the Naryn River. The high shorelines (1850 m to 1735 m) show a period of stable water levels followed by a slow phase of regression, which is also notable for the large Issyk-Kul lake during the same time period (Burgette et al., 2017). This regression continued until the lake was suddenly emptied, as recorded by the HFE unit.

The second lake was established for a minimum period of 7675 ± 1285 yrs., recording another long residence time. The highest shorelines inferred for this lake (light blue line at 1720 m in Fig. 2a) outline a 72 km-long and 15 km-wide lake (~455 km^2) and a volume of 27 ± 10 km^3 (calculated with QGIS and a DEM of the current topography). For this second lake, morphological and sedimentological observations revealed a lower stable lake level between 1715 m and 1695 m, followed by episodic emptying phases. Indeed, we suspect successive drops of the lake level from 1695 m to 1650 m, and then a late stable water level at 1650–1630 m, but with no age constraint. This final lake stage ended with the total drainage of the basin when the Naryn River incised again to retrieve its base level. An explanation for the long stability and drainage may be found by resurgence in the dam which allows water to be released and to balance out the water pressure on the dam as proposed for the modern Usoi dam in Tadjikistan (Ischuk, 2006; Delaney and Evans, 2011).

Both residence times are much longer than previously proposed (Fan et al., 2020) but are still in the range of other large landslide-dammed lakes worldwide such as the Aricota Lake (Peru), formed by a 600 m-high dam that formed a 6 km-long lake which persisted for 18,000 years (Delgado et al., 2020), the Green Lake (New Zealand), with a 800 m-high dam, impounding a lake of 11 km-long which remained stable for 13,000 years (Hancox and Perrin, 2009), or the Lulang Lake (Tibet) formed by a 100 m-high dam, impounding a 2.5 km-long lake with a residence time of 9200 years (Wang et al., 2019). However, our study shows that the first dam lake is the most durable lake in comparison with all other examples described in the literature so far. The long retention time of the lake thus represents a greater danger in the event of a dam failure. In addition, it must have had major consequences for the area, such as the intensive modification of the drainage system of the catchment area, the modification of the environment for various species or the absence of water resources downstream in the long term. However, no downstream morphological markers have yet been found to support the rebalancing of the river system and the modification of the catchment basins due to the river damming or to the drainage of the lakes.

5.2. Quantification of filling and draining times

Classically, the flow of a river, and thus the filling rate of a natural lake, is directly proportional to the size of the upstream drainage area (Costa and Schuster, 1988). Here, we used the current baseflow of the Naryn River of 200 ± 50 m^3/s (State Water Inventory, Strom, 2010) to determine an approximate filling time for both lakes, according to:

$$t = \frac{V}{Q} \tag{1}$$

with V the volume of the lake in m^3 and Q the flow of the river in m^3/s. For the first lake, we assume that the highest water level at 1850 m was promptly reached for a total volume of 121 ± 50 km^3, yielding a filling time of 19.2 ± 12 years. For the second lake we propose a high lake level at 1720 m and a volume of 27 ± 10 km^3, with a filling period of 4.3 ± 2 years. These filling periods could have been longer if the flow of the Naryn River had been lower than the present one and if the lake filled more gradually. These filling times are similar to the one of Lake Sarez (Tajikistan) which may be seen as an analogue of the Beshkiol case. In fact, Sarez Lake reached a first level of 400 m in 15 years approximately and about 500 m in 1944 (Ischuk, 2006; Delaney and Evans, 2011). It is also possible to compare the filling times of the Beshkiol lakes with those of anthropogenic dam lakes. The Toktugul dam lake (Kyrgyzstan), built further downstream on the Naryn River, took two years to reach a height of 100 m (Simpson et al., 1981). In addition, the Three Gorges Reservoir (China) filled in five years with 40 km^3 (Tang et al., 2019) or the Kariba Lake (Zambia/Zimbabwe) filled in five years with 160 km^3 (Marshall, 1988).

Dam failures are often associated with catastrophic flooding downstream (Hewitt, 1998; Nash et al., 2008). According to O'Connor and Costa (2004), the greater the height of a landslide dam, the greater the potential peak discharge through the dam, exponentially. Therefore, it is in narrow valleys, where landslides form high dams, that we can find the greatest potential for extreme flooding. Based on satellite imagery analysis, no evidence of catastrophic flooding deposits has yet been observed downstream of the Beshkiol area but our sedimentological investigations across the Naryn Basin favour a rapid catastrophic discharge (HFE unit) of the first lake. We calculated the time needed to empty the lake in a drastic way, using a classical formula (demonstration in supplementary material S2) with:

$$t = \frac{2A}{\kappa S} \times \sqrt{\frac{h}{2g}} \tag{2}$$

where A is the surface of the lake, S is the orifice area (km^2), $\kappa = 0.62$, $g = 9.81$ m/s^2, and h is the water height (m). For the first dam, we have calculated a lake surface of ~1100 km^2 and estimated the lake depth to be 350 ± 10 m. Using the current topography and different geometries for the dam breach, we calculated an orifice between 0.28 km^2 and 0.07 km^2, which would allow the first lake to drain in 15 h to 55.2 h. This time range is comparable to the largest outburst events recorded in historical time. The biggest outburst event is the First Great Indus Flood (Pakistan, 1841), with a lake of 65 km-long catastrophically drained in a period of about 24 h (Delaney and Evans, 2011). The 2000 Yigong event

is the second largest outburst ever recorded, with a 48.9 km^2 lake surface entirely drained in about 12 h (Delaney and Evans, 2015).

5.3. What triggered the landslides?

5.3.1. First landslide

Landslide triggers can be both seismic and climatic (Xu et al., 2009; Pánek, 2015), but the exceptional dimensions of the Beshkiol Landslide (8–12 km^3, a runout of 10 km, a fall height of 2.4 km) likely support a seismic origin. In steep topography environments, earthquake-triggered landslides occur when the horizontal peak ground acceleration exceeds 0.2 g, typically acceleration values reached in regions exposed to intensities greater than VII (Wald et al., 1999; Meunier et al., 2007). Considering that the Beshkiol Landslide is located close or in continuation of traces of crustal active faults (Strom, 1998; Thompson et al., 2002; Goode et al., 2014; Rizza et al., 2019), a co-seismic triggering of the slope failures is favoured. The best candidate is the normal fault system running from Kazarman to the Beshkiol body (Rizza et al., 2019), also evidenced by a cluster of landslides (Chaartash rock avalanches) observed along the westhern slope of the Akshiyriak Range (Strom, 1998; Havenith et al., 2015). Within 10 km of Beshkiol, other faults in the Naryn Basin are mapped with segments of several tens of kilometres long and can therefore generate Mw > 7 earthquakes (Fig. 2). However, any paleoseismic record, as old as the Beshkiol slope failures, does exist for the moment that would corroborate a co-seismic trigger.

Another trigger could be the incision of the Naryn River associated with the long-term uplift of the range, which may have steepened the relief and in this case the topography is probably the first preconditioning factor for the giant gravitational failures found at Beshkiol. In addition, the lithology with the presence of gypsum beds found in the Chu Formation may have played the role of a décollement layer and would have facilitated landslides. Finally, climatic factors may also play an important role in the triggering of the landslides during wet or glacial periods (Trauth et al., 2003; Crozier, 2010). However, between 56,275 and 47,485 years, no particular wet conditions were recorded in the region (Cheng et al., 2012; Li et al., 2020). For this reason, the climatic factor is the less favoured trigger for the initiation of the giant landslide.

5.3.2. Second landslide

A second dam episode occurred <1490 yrs after the drainage of the first lake, implying short-term slope destabilisation. Our interpretation is that the distal part of the main body (secondary scars, Fig. 5) observed in the topography, which could mark the edge of the Naryn paleo-valley after erosion of the first dam, is the place of initiation of a large secondary landslide-dams. Deep regressive erosion and gravity effect occurred, due to the fast incision of the Naryn River to recover a base level after the drainage of the first lake. Moreover, between 13 kyrs and 15 kyrs, this part of the Tien Shan was impacted by an increase in precipitations (Li et al., 2020). This period is synchronous with the sudden breach of the first dam at Beshkiol and with a period of deep incision within the Naryn lake sediments (erosional surface 2, Fig. 3) that was shortly followed by the formation of a second dam. Furthermore, during this period, alluvial fan aggradation is recorded at Jangy-Talap, while 50 km upstream, alluvial fans are abandoned at 14,120–14,695 yrs. cal BP (yellow star in Fig. 2a, recalibrated after Thompson et al., 2002) and are incised by narrow gorges. This large fan aggradation phase and subsequent incision are widely recorded in the Kyrgyz range between 15.5 and 13.5 kyrs within the different intramontane basins (Thompson et al., 2002; Burgette et al., 2017), suggesting a potential global climatic impact on the lake filling, dam stability and river incision. Finally, an earthquake associated with an extreme climatic event would be enough to trigger landslides that would cause a second dam episode, a hypothesis that cannot be solved currently due to the scarce paleoclimatic and paleoseismic records.

5.3.3. Future failures potential

The distal part of the Beshkiol Landslide, made of unconsolidated Chu Formation, is characterized by large, steep cliffs plunging into the Naryn River. The "void" created by the incision of the Naryn River could facilitate the fall of blocks and small volumes of unconsolidated sediments, especially during seismic shaking, which may still create dams but probably with lower heights and shorter residence times. Nevertheless, the observation of open, extensive fractures along the secondary scars in the Chu Formation, indicates that significant masses of material appear to be unstable and close to failure. In the event of an earthquake and/or extreme rain episode, one or more new landslides could initiate from these fragilities and potentially cause damming of the Naryn River.

6. Conclusion

The Beshkiol Landslide, the biggest one in Central Asia, was triggered during the late Pleistocene and dammed the Naryn River for an extensive period of time. Two large lakes had occupied the Naryn Basin during long periods of 36,980 ± 5140 yrs. and 7675 ± 1285 yrs., and the basin was only drained shortly between 15,645 and 14,155 cal BP, after a catastrophic outburst event. Our study emphasises that landslide triggered dams and their associated lakes can be maintained for several tens of thousand years and such long-lived stability may have significantly controlled the hydrology and the fluvial aggradation on a rather large area. The Beshkiol-Naryn region is located in an active tectonic zone where large earthquakes are expected to occur and where drastic changes in precipitation are forecasted in response to ongoing climate changes. Large destabilized volumes on the distal part of the Beshkiol Landslide could be remobilized during extreme events (earthquake or rainfall), causing a potentially major damming of the Naryn River with significant regional economic repercussions, such as a reduction in the hydroelectric production of Kyrgyzstan.

Credit authorship contribution statement

J. Losen: Formal analysis, Investigation, Methodology, Writing – original draft. **M. Rizza:** Formal analysis, Funding acquisition, Investigation, Supervision, Writing – original draft. **A. Nutz:** Formal analysis, Investigation, Writing – original draft. **M. Henriquet:** Investigation, Writing – original draft. **M. Schuster:** Investigation, Writing – original draft. **E. Rakhmedinov:** Investigation, Writing – original draft. **S. Baikulov:** Investigation, Writing – original draft. **K. Abdrakhmatov:** Investigation. **J. Fleury:** Formal analysis. **L. Siame:** Supervision, Writing – original draft.

Declaration of competing interest

The authors declare that they have no known competing financial interests or personal relationships that could have appeared to influence the work reported in this paper.

Data availability

Data will be made available on request.

Acknowledgments

This work was supported by the Centre National d'Etudes Spatiales CNES (HIDATHSA project). Pléiades images are provided by the CNES in the framework of ISIS Programme. This project has received funding from "Excellence Initiative" of Aix Marseille University A*MIDEX, a french "Investissement d'avenir" program. We thank the LMC14 staff (Laboratoire de Mesure du Carbone-14), ARTEMIS national facility, (LSCE-(CNRS-CEA-UVSQ)-IRD-IRSN-MC) for the results obtained with the accelerator mass spectrometry method. This research was partly run under support from the NATO Science for Peace and Security Program

through Multi-year project G5690. We would like to thank the reviewers for taking the time to correct our manuscript and for their pertinent comments and criticisms, as well as V. Rinterknecht, who revised our manuscript, checked and improving for English quality. We are grateful to Ian Pierce and Ramon Arrowsmith who have taken aerial pictures in the Naryn Basin using a drone in summer 2021. We thank all those involved in the 2021 and 2022 field seasons, in particular Anaigul for her efficient camp management and amazing food; our drivers Munduz, Genia and Ruslan. The data used in this study are available in the tables.

Appendix A. Supplementary data

Supplementary data to this article can be found online at https://doi.org/10.1016/j.geomorph.2024.109121.

References

Abdrakhmatov, K.Y., Weldon, R., Thompson, S.C., Burbank, D.W., Rubin, C., Miller, M., Molnar, P., 2001. Origin, direction, and rate of modern compression in the central Tien Shan, Kyrgyzstan. Geol. Geofiz. 42, 1585–1609.

Adamiec, G., Aitken, M.J., 1998. Dose-rate conversion factors: update. Ancient tL 16 (2), 37–50.

Alden, W.C., 1928. Landslide and flood at Gros Ventre, 140. Amer. Inst. Min. and Met. Eng., Technical Publication, Wyoming, pp. 1–14.

Burgette, R.J., Weldon II, R.J., Abdrakhmatov, K.Y., Ormukov, C., Owen, L.A., Thompson, S.C., 2017. Timing and process of river and lake terrace formation in the Kyrgyz Tien Shan. Quat. Sci. Rev. 159, 15–34.

Cartigny, M.J., Postma, G., Van den Berg, J.H., Mastbergen, D.R., 2011. A comparative study of sediment waves and cyclic steps based on geometries, internal structures and numerical modeling. Mar. Geol. 280 (1–4), 40–56.

Cartigny, M.J., Ventra, D., Postma, G., van Den Berg, J.H., 2014. Morphodynamics and sedimentary structures of bedforms under supercritical-flow conditions: new insights from flume experiments. Sedimentology 61 (3), 712–748.

Cheng, H., Zhang, P.Z., Spötl, C., Edwards, R.L., Cai, Y.J., Zhang, D.Z., Sang, W.C., Tan, M., An, Z.S., 2012. The climatic cyclicity in semiarid-arid Central Asia over the past 500,000 years. Geophys. Res. Lett. 39 (1) https://doi.org/10.1029/2011GL050202.

Costa, J.E., Schuster, R.L., 1988. The formation and failure of natural dams. Geol. Soc. Am. Bull. 100 (7), 1054–1068.

Crozier, M.J., 2010. Deciphering the effect of climate change on landslide activity: a review. Geomorphology 124 (3–4), 260–267.

Delaney, K.B., Evans, S.G., 2011. Rockslide Dams in the Northwest Himalayas (Pakistan, India) and the Adjacent Pamir Mountains (Afghanistan, Tajikistan), Central Asia. Nat. Artif. Rockslide Dams 205–242.

Delaney, K.B., Evans, S.G., 2015. The 2000 Yigong landslide (Tibetan Plateau), rockslide-dammed lake and outburst flood: Review, remote sensing analysis, and process modelling. Geomorphology 246, 377–393.

Delgado, F., Zerathe, S., Audin, L., Schwartz, S., Benavente, C., Carcaillet, J., Aster Team, 2020. Giant landslide triggerings and paleoprecipitations in the Central Western Andes: the aricota rockslide dam (South Peru). Geomorphology 350, 106932.

Delvaux, D., Abdrakhmatov, K.E., Lemzin, I.N., Strom, A.L., 2001. Landslides and Surface Breaks of the 1911 Ms 8.2 Kemin Earthquake, Kyrgyzstan.

Dumoulin, J.P., Comby-Zerbino, C., Delqué-Količ, E., Moreau, C., Caffy, I., Hain, S., Beck, L., 2017. Status report on sample preparation protocols developed at the LMC14 Laboratory, Saclay, France: from sample collection to 14C AMS measurement. Radiocarbon 59 (3), 713–726.

Durcan, J.A., King, G.E., Duller, G.A., 2015. DRAC: Dose Rate and Age Calculator for trapped charge dating. Quat. Geochronol. 28, 54–61.

Ermini, L., Casagli, N., 2003. Prediction of the behaviour of landslide dams using a geomorphological dimensionless index. Earth Surf. Process. Landf. 28 (1), 31–47. The Journal of the British Geomorphological Research Group.

Evans, S.G., Hermanns, R.L., Strom, A., Scarascia-Mugnozza, G., (Eds.)., 2011. Natural and Artificial Rockslide Dams, vol. 133. Springer Science & Business Media.

Fan, X., Dufresne, A., Subramanian, S.S., Strom, A., Hermanns, R., Stefanelli, C.T., Xu, Q., 2020. The formation and impact of landslide dams–State of the art. Earth Sci. Rev. 203, 103116.

Galbraith, R.F., Roberts, R.G., 2012. Statistical aspects of equivalent dose and error calculation and display in OSL dating: An overview and some recommendations. Quat. Geochronol. 11, 1–27.

Goode, J.K., Burbank, D.W., Bookhagen, B., 2011. Basin width control of faulting in the Naryn Basin, south-Central Kyrgyzstan. Tectonics 30 (6).

Goode, J.K., Burbank, D.W., Ormukov, C., 2014. Pliocene-Pleistocene initiation, style, and sequencing of deformation in the central Tien Shan. Tectonics 33 (4), 464–484.

Goswami, U., Sarma, J.N., Patgiri, A.D., 1999. River channel changes of the Subansiri in Assam, India. Geomorphology 30 (3), 227–244.

Grützner, C., Walker, R., Ainscoe, E., Elliott, A., Abdrakhmatov, K., 2019. Earthquake environmental effects of the 1992 MS7. 3 Suusamyr earthquake, Kyrgyzstan, and their implications for Paleo-earthquake studies. Geosciences 9 (6), 271.

Guérin, G., Mercier, N., Nathan, R., Adamiec, G., Lefrais, Y., 2012. On the use of the infinite matrix assumption and associated concepts: a critical review. Radiat. Meas. 47 (9), 778–785.

Guérin, G., Christophe, C., Philippe, A., Murray, A.S., Thomsen, K.J., Tribolo, C., Lahaye, C., 2017. Absorbed dose, equivalent dose, measured dose rates, and implications for OSL age estimates: introducing the Average Dose Model. Quat. Geochronol. 41, 163–173.

Hancox, G.T., Perrin, N.D., 2009. Green Lake Landslide and other giant and very large postglacial landslides in Fiordland, New Zealand. Quat. Sci. Rev. 28 (11–12), 1020–1036.

Havenith, H.B., Abdrakhmatov, K., Torgoev, I., Ischuk, A., Strom, A., Bystrický, E., Cipciar, A., 2013. Earthquakes, landslides, dams and reservoirs in the Tien Shan, Central Asia. In: Landslide Science and Practice: Volume 6: Risk Assessment, Management and Mitigation, pp. 27–31.

Havenith, H.B., Strom, A., Torgoev, I., Torgoev, A., Lamair, L., Ischuk, A., Abdrakhmatov, K., 2015. Tien Shan geohazards database: Earthquakes and landslides. Geomorphology 249, 16–31.

Hawker, L., Uhe, P., Paulo, L., Sosa, J., Savage, J., Sampson, C., Neal, J., 2022. A 30 m global map of elevation with forests and buildings removed. Environ. Res. Lett. 17 (2), 024016.

Hewitt, K., 1998. Catastrophic landslides and their effects on the Upper Indus streams, Karakoram Himalaya, northern Pakistan. Geomorphology 26 (1–3), 47–80.

Ischuk, A.R., 2006. Usoy natural dam: Problem of security; Lake Sarez, Pamir Mountains, Tadjikistan. Ita. J. Eng. Geol. Environ. (special issue 1), 189–192. https://doi.org/10.4408/IJEGE.2006-01.S-26.

Kalmetieva, Z.A., Mikolaichuk, A.V., Moldobekov, B.D., Meleshko, A.V., Jantaev, M.M., Zubovich, A.V., Havenith, H.B., 2009. Atlas of earthquakes in Kyrgyzstan. In: CAIAG, Bishkek, 76.

Korup, O., Strom, A.L., Weidinger, J.T., 2006. Fluvial response to large rock-slope failures: examples from the Himalayas, the Tien Shan, and the Southern Alps in New Zealand. Geomorphology 78 (1–2), 3–21.

Kreutzer, S., Burow, C., Dietze, M., Fuchs, M.C., Schmidt, C., Fischer, M., Fuchs, M., 2016. Luminescence: comprehensive luminescence dating data analysis. https://doi.org/10.5281/zenodo.8221196.

Lebrun, B., Frerebeau, N., Paradol, G., Guérin, G., Mercier, N., Tribolo, C., Rizza, M., 2020. Gamma: An R Package for Dose Rate Estimation from In-Situ Gamma-Ray Spectrometry Measurements. Ancient TL 38 (2), 1–5. https://hal.science/hal-03019182.

Li, Y., Song, Y., Orozbaev, R., Dong, J., Li, X., Zhou, J., 2020. Moisture evolution in Central Asia since 26 ka: Insights from a Kyrgyz loess section, Western Tian Shan. Quat. Sci. Rev. 249, 106604.

Liritzis, I., Stamoulis, K., Papachristodoulou, C., Ioannides, K., 2013. A re-evaluation of radiation dose-rate conversion factors. Mediter. Archaeol. Archaeom. 13 (3), 1–15.

Marshall, B.E., 1988. Seasonal and annual variations in the abundance of pelagic sardines in Lake Kariba, with special reference to the effects of drought. Arch. Hydrobiol. 399–409.

Meunier, P., Hovius, N., Haines, A.J., 2007. Regional patterns of earthquake-triggered landslides and their relation to ground motion. Geophys. Res. Lett. 34 (20).

Mook, W.G., Van Der Plicht, J., 1999. Reporting 14C activities and concentrations. Radiocarbon 41 (3), 227–239.

Moreau, C., Caffy, I., Comby, C., Delqué-Količ, E., Dumoulin, J.P., Hain, S., Vincent, J., 2013. Research and development of the Artemis 14C AMS Facility: status report. Radiocarbon 55 (2), 331–337.

Morino, C., Conway, S.J., Sæmundsson, Þ., Helgason, J.K., Hillier, J., Butcher, F.E., Argles, T., 2019. Molards as an indicator of permafrost degradation and landslide processes. Earth Planet. Sci. Lett. 516, 136–147.

Murray, A., Arnold, L.J., Buylaert, J.P., Guérin, G., Qin, J., Singhvi, A.K., Thomsen, K.J., 2021. Optically stimulated luminescence dating using quartz. Nat. Rev. Methods Primers 1 (1), 72.

Nash, T., Bell, D., Davies, T., Nathan, S., 2008. Analysis of the formation and failure of Ram Creek landslide dam, South Island, New Zealand. N. Z. J. Geol. Geophys. 51 (3), 187–193.

O'Connor, J.E., Costa, J.E., 2004. The world's Largest Floods, Past and Present: Their Causes and Magnitudes (No. 1254). US Geological Survey.

Pánek, T., 2015. Recent progress in landslide dating: a global overview. Prog. Phys. Geogr. 39 (2), 168–198.

Ramsey, C.B., 2008. Radiocarbon dating: revolutions in understanding. Archaeometry 50 (2), 249–275.

Ramsey, C.B., 2009. Bayesian analysis of radiocarbon dates. Radiocarbon 51 (1), 337–360.

Reimer, P.J., Austin, W.E., Bard, E., Bayliss, A., Blackwell, P.G., Ramsey, C.B., Talamo, S., 2020. The IntCal20 Northern Hemisphere radiocarbon age calibration curve (0–55 cal kBP). Radiocarbon 62 (4), 725–757.

Rizza, M., Abdrakhmatov, K., Walker, R., Braucher, R., Guillou, V., Carr, A.S., Keddadouche, K., 2019. Rate of slip from multiple Quaternary dating methods and paleoseismic investigations along the Talas-Fergana Fault: Tectonic implications for the Tien Shan Range. Tectonics 38 (7), 2477–2505.

Rupnik, E., Daakir, M., Pierrot Deseilligny, M., 2017. MicMac–a free, open-source solution for photogrammetry. Open Geospatial Data, Software and Standards 2 (1), 1–9. https://doi.org/10.1186/s40965-017-0027-2.

Schuster, R.L., Alford, D., 2004. Usoi landslide dam and lake sarez, Pamir mountains, Tajikistan. Environ. Eng. Geosci. 10 (2), 151–168.

Simpson, D.W., Hamburger, M.W., Pavlov, V.D., Nersesov, I.L., 1981. Tectonics and seismicity of the Toktogul reservoir region, Kirgizia, USSR. J. Geophys. Res. Solid Earth 86 (B1), 345–358.

Strom, A., 2010. Landslide dams in Central Asia region. J. Jpn. Landslide Soc. 47 (6), 309–324.

Strom, A.L., 1998. Giant ancient rock slides and rock avalanches in the Tien Shan Mountains, Kyrgyzstan. Landslide News 11, 20–23.

Strom, A.L., Korup, O., 2006. Extremely large rockslides and rock avalanches in the Tien Shan Mountains, Kyrgyzstan. Landslides 3 (2), 125–136.
Tang, H., Wasowski, J., Juang, C.H., 2019. Geohazards in the three Gorges Reservoir Area, China–Lessons learned from decades of research. Eng. Geol. 261, 105267.
Tapponnier, P., Molnar, P., 1979. Active faulting and Cenozoic tectonics of the Tien Shan, Mongolia, and Baykal regions. J. Geophys. Res. Solid Earth 84 (B7), 3425–3459.
Thompson, S.C., Weldon, R.J., Rubin, C.M., Abdrakhmatov, K., Molnar, P., Berger, G.W., 2002. Late Quaternary slip rates across the central Tien Shan, Kyrgyzstan, Central Asia. J. Geophys. Res.: Solid Earth 107 (B9), ETG-7.
Trauth, M.H., Bookhagen, B., Marwan, N., Strecker, M.R., 2003. Multiple landslide clusters record Quaternary climate changes in the northwestern argentine Andes. Palaeogeogr. Palaeoclimatol. Palaeoecol. 194 (1–3), 109–121.
Wald, D.J., Quitoriano, V., Heaton, T.H., Kanamori, H., Scrivner, C.W., Worden, C.B., 1999. TriNet "ShakeMaps": Rapid generation of peak ground motion and intensity maps for earthquakes in southern California. Earthq. Spectra 15 (3), 537–555.
Wang, H., Cui, P., Liu, D., Liu, W., Bazai, N.A., Wang, J., Lei, Y., 2019. Evolution of a landslide-dammed lake on the southeastern Tibetan Plateau and its influence on river longitudinal profiles. Geomorphology 343, 15–32.
Weidinger, J.T., 2011. Stability and life span of landslide dams in the Himalayas (India, Nepal) and the Qin Ling Mountains (China). Nat. Artif. Rockslide Dams 243–277.
Weng, M.C., Wu, M.H., Ning, S.K., Jou, Y.W., 2011. Evaluating triggering and causative factors of landslides in Lawnon River Basin, Taiwan. Eng. Geol. 123 (1–2), 72–82.
Wintle, A.G., 1997. Luminescence dating: laboratory procedures and protocols. Radiat. Meas. 27 (5–6), 769–817.
Wintle, A.G., Murray, A.S., 2000. Quartz OSL: effects of thermal treatment and their relevance to laboratory dating procedures. Radiat. Meas. 32 (5–6), 387–400.
Xu, Q., Fan, X.M., Huang, R.Q., Westen, C.V., 2009. Landslide dams triggered by the Wenchuan Earthquake, Sichuan Province, South West China. Bull. Eng. Geol. Environ. 68, 373–386.
Yi, X., Feng, W., Bai, H., et al., 2021. Catastrophic landslide triggered by persistent rainfall in Sichuan, China: August 21, 2020, Zhonghaicun landslide. Landslides 18, 2907–2921.